Journal of
Nanoscience and Nanotechnology
Vol. 11, 1–7, 2011

Spreading Characteristics of Nanofluid Droplets Impacting onto a Solid Surface

S. M. Sohel Murshed* and C. A. Nieto de Castro

Centro de Ciências Moleculares e Materiais, Faculdade de Ciências, Universidade de Lisboa, Campo Grande, 1749-016 Lisboa, Portugal

This paper reports an experimental investigation on the spreading characteristics of nanofluid droplets impinging on aluminum substrate under the influence of several key factors such as nanoparticle volume fraction, substrate temperature, and the Weber number. Sample nanofluid used is prepared by dispersing several volumetric concentrations (1 to 5%) of titanium dioxide nanoparticles in ethylene glycol. The entire dynamic process of each droplet collision with the substrate surface and the spreading phenomena is captured by using a high speed camera and then the transient spreading diameter and height of droplet are determined. It is found that the higher the concentration of nanoparticles the larger the spreading diameter of nanofluid droplet. As the surface temperature increases, the overall spreading diameter and height of nanofluid droplet significantly decreases and increases, respectively. At larger Weber number, the final spreading of the nanofluid droplet is also found to be larger than that of lower Weber number. Present results demonstrate that spreading characteristics of nanofluid droplets impacting onto solid surface are greatly influenced by each of the aforementioned factors.

Keywords: Nanofluids, Nanoparticles, Droplet, Spreading, Substrate, Temperature.

RESEARCH ARTICLE

1. INTRODUCTION

The advances in nanotechnology particularly production of nanoparticulates have brought about the development of new class of heat transfer fluids termed as nanofluids which was coined at Argonne national laboratory of USA in 1995.[1] Nanofluids are engineered by dispersing nanometer-sized metallic or nonmetallic particles or tubes in conventional heat transfer fluids such as water, ethylene glycol, and engine oil. Nanofluids have attracted great interest from the research community due to their enhanced thermophysical properties, potential benefits and application in numerous industries such as microelectronics, transportation, biomedical, HVAC and so on. Researchers found that nanofluids exhibit much higher thermal conductivities than the base fluids themselves and they are considered to be the next generation coolant for microelectronics and other advanced cooling techniques.[2–7] Most of the reported research efforts mainly focused on the effective thermal conductivity, convective and boiling heat transfer of nanofluids. The dynamics of single-phase (non-boiling) and two-phase (boiling) liquid droplets impinging on various surfaces have extensively been studied as the spreading of liquid droplet plays a key role in many industrial processes like spray cooling, coating, ink-jet printing, and oily soil removal.[8–15] However, very little work has been performed on the droplet behavior of nanofluids upon impinging on a solid surface. Besides fascinating thermophysical and heat transfer properties, studies on boiling heat transfer of nanofluids indicated that nanofluids could be very promising for enhanced spray cooling systems.[16–19] Thus, it is of great importance to investigate impingement of nanofluids droplets on heated substrate surface for their applications in aforementioned industrial processes, particularly in spray cooling and coating.

In studying the impact behavior of water droplets on a heated (100 to 280 °C) polished aluminum surface, Bernardin et al.[10] found that each boiling heat transfer regime possesses individual, temperature-dependent droplet impact characteristics and that the Weber number strongly influences these characteristics. In all boiling regimes, they observed that with increasing Weber number both the spreading ratio and the instabilities responsible for droplet breakup also increase and that lower temperatures lead to higher spreading ratio particularly in the nucleate boiling regime. In another similar study, the same research group[20] further investigated the temperature dependence of the quasi-static contract angle of water droplets on a

*Author to whom correspondence should be addressed.

polished aluminum surface for various surface temperatures between 25 to 170 °C and pressures between 101.3 to 827.4 kPa. They reported two distinct temperature-dependent regimes where a relatively constant contract angle of 90° was observed at temperature, $T < 120$ °C and the contract angle decreased fairly linear manner at $T > 120$ °C. However, no pressure dependence of the contract angle was observed. Later Kandlikar and Steinke[13] studied the effect of surface roughness and temperature on contact angle of droplet at constant Weber number. The effect of temperature on dynamic and receding contact angle was observed only at temperature range of 140–150 °C. They presumed that at this temperature, rapid evaporation near the liquid–solid contact region influences the dynamic contact angles and both dynamic advancing and receding contact angles become almost the same. Using high speed photography, Manzello and Yang[14] conducted experiments on the impact of distilled water droplet upon a heated wax surface. The Weber number was varied at a temperature range of 20–75 °C. They reported that the liquid films recoil faster as the surface temperature was increased. Although some instabilities were reported for droplet impingement at Weber number of 150 and no considerable influence of surface temperature was observed. Using molecular dynamics simulation Heine et al.[21] the spreading of liquid nanodroplets of different initial radii and they found droplet sized-dependent effective diffusion coefficient.

Among very few studies, Wasan and Nikolov[22] were the first to investigate the effects of the particle structure formation and the structural disjoining pressure of nanoparticles on the spreading of nanofluids on solid surface. Their results indicate that the in-layer particle structuring can enhance the spreading of nanofluids on solids. Recently, Duursma et al.[23] studied the effect of aluminum nanoparticles on droplets boil-off by allowing nanofluid drops to fall onto a copper surface at temperature higher than the liquid saturation temperature. The droplet behavior and heat flux were investigated against to those of base fluids used i.e., water, ethanol, and dimethyl sulfoxide (DMSO). They demonstrated that increasing the surface temperature and Weber number promote the receding breakup scenario, while increasing the nanoparticle concentration discourages this breakup. Except DMSO nanofluids, they however, did not find any significant enhancement in the heat fluxes associated with base fluids and other nanofluids droplets. Shen et al.[24] very recently investigated the influence of surface temperature on the hydrodynamic characteristics of water and a nanofluid droplets impinging on a polished and nanostructured surface. In their experiments, a nanofluid containing 0.2 weight% of single wall carbon nanotubes (SWCNT) in deionized water was used at various surface temperatures ranging from 25 to 185 °C. Their results showed that nanofluid has larger spreading diameter compared to that of that of deionized water and using a nanofluid or a nanostructured surface can reduce the total evaporation time up to 20% and 37%, respectively. Nevertheless, no effort was made to study the effect of other important factors such as nanoparticle concentration and Weber number on these hydrodynamic characterisitics of droplets.

In this study, spreading characteristics of nanofluid droplets impacting onto a solid surface under the influence of several nanoparticle volume fractions, various substrate temperatures (non-heating and non-boiling temperatures), and different Weber numbers are investigated.

2. CHARACTERIZATION OF SAMPLE NANOFLUID

Sample nanofluids are prepared by suspending several volumetric concentrations ($\phi_{np} = 0.01$ to 0.05) of TiO_2 nanoparticles of 15 nm diameter in ethylene glycol. Ethylene glycol was used as base fluid because it has much higher boiling point (~200 °C) than that of water and nanoparticles were found to be well dispersed in this fluid. In order to prepare proper sample nanofluids, well mixing and stabilization of suspended nanoparticles are essential. Prior to experiments sample nanofluids must be properly homogenized to ensure very good dispersion of nanoparticles in base fluid. Thus an ultrasonic dismenbrator is used for 4 to 5 hours to obtain well-homogenized suspensions of nanoparticles. In order to obtain the desired Weber number for droplets with 1% volumetric concentration of nanoparticles, the surface tension of this nanofluid was measured and found to be 42.3 mN/m which is lower than the standard value (47.99 mN/m) of surface tension of ethylene glycol at room temperature.[25] Similar reduction of surface tension of deionized water was previously reported when a low volume-fractioned TiO_2 nanoparticles was dispersed in it.[26] Since density of this nanofluid (1 volume%) is not available, it is determined by using volume fraction mixture rule and is found to be 1140 kg/m^3.

3. EXPERIMENTAL SETUP AND PROCEDURE

An experimental facility was established to investigate the spreading characteristics of nanofluid droplets impinging on a solid surface. The experimental setup consists of several major components such as substrate, heating system, thermocouple, drop delivery system, high speed camera and data acquisition system. A schematic of the experimental system is shown in Figure 1. An aluminum smooth substrate surface of 2 inches diameter size was used which was heated using a rod-heater inserted from the bottom of the substrate. The heater was connected with a Power supply (BK Precision Co.). A K-type calibrated microthermocouple was used to read the surface temperature. The drop delivery system is made using of a precision

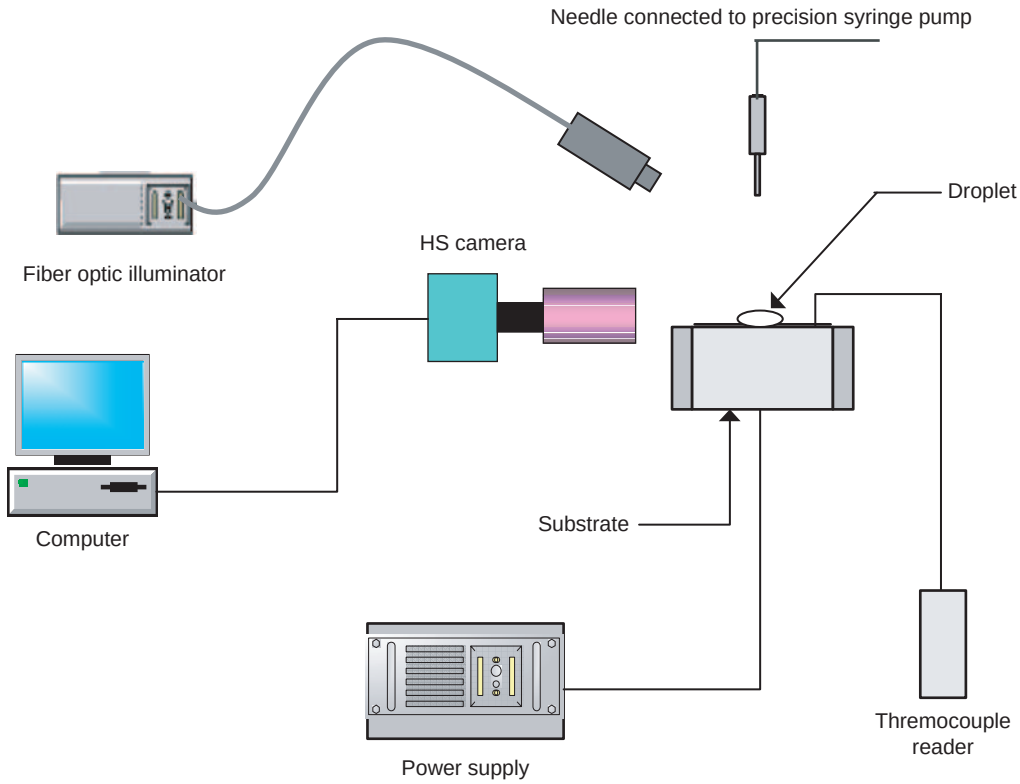

Fig. 1. Schematic of experimental setup.

syringe pump (KD Scientific Inc., USA) and tubing connected to micron-sized needle clamped above the substrate. Thus, the volume and size of the droplet released were accurately controlled and the height of the needle tip can easily adjust to obtain various droplet releasing heights (s). The droplet release height (s) was varied between 10 cm to 40 cm from the substrate surface.

The complete droplet impingement and spreading process on the substrate surface was recorded using a high speed camera (Prosilica Inc.) at a rate of 500 frames per second (fps). A close-up lens was used to magnify and focus the sharp images of the impacted droplet. Dual fiber optic light guide (150 Watts fiber optic illuminator) was used to provide sufficient illumination at the droplet impact area on the substrate surface. Image acquisition and camera controlling were performed using ProStream recording software. Recorded images were then post-processed using a customized Mathlab program and Windig digitalization software to determine the initial droplet size, droplet spreading diameter and height after impingement. The captured needle (known size) image served as a reference scale for the analysis of the droplet dimensions.

4. RESULTS AND DISCUSSION

The transient spreading diameter and height of droplet are two most important parameters to characterize droplet impingement dynamics and subsequent heat transfer. Experimental results are characterized using these two time-dependent nondimensional spreading parameters (i.e., droplet diameter and height) as individual function of volumetric concentration of nanoparticles, substrate surface temperature (both non-heating and non-boiling conditions), and the Weber number. Both the spreading diameter and the height of droplet which are non-dimensionalized by the pre-impact droplet diameter (D) are expressed by $d^* = d/D$ and $h^* = h/D$, respectively where d is the droplet diameter after impact and h is the height of the droplet after impact. Figure 2 depicts all droplet

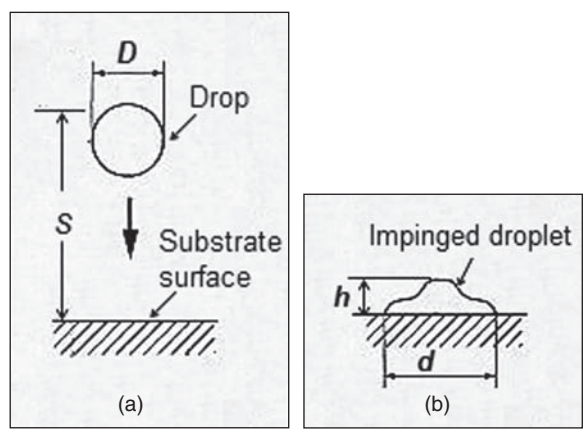

Fig. 2. Illustration of droplet parameters (a) before and (b) after impacting the surface.

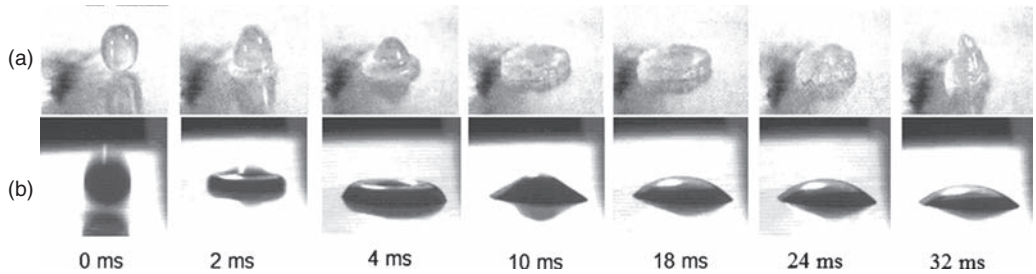

Fig. 3. Sequential nanofluid droplet morphology at releasing height of 10 cm and surface temperature of 130 °C for (a) $\phi_{np} = 0.01$ and (b) $\phi_{np} = 0.05$.

parameters before and after impacting the surface. The time is set to be zero ($t = 0$) at the moment of impact. However as it was difficult to capture the image of a droplet just exactly at the moment of coming into contact with the surface, some data of sequential droplet spreading diameter and height are not plotted from zero time. The sequential droplet spreading and height are determined starting from the impact time ($t = 0$) and except for the case of varying Weber number, they are presented in the form of nondimensional time, $t^* = tV_0/D$ where V_0 is the impact velocity of the droplet. In the present experiments, the diameter of the droplet prior to impact (D) was tried to maintained constant value of 1.4 mm.

4.1. Effect of Nanoparticles Concentration

Figure 3 depicts sequence of images of nanofluid droplet showing collision and spreading for two different volume factions of nanoparticles. It can be seen that right after the impact droplets spreading advance drastically (this stage can be termed as initial spreading) followed by partial rebound (termed as rebounding or retraction) and subsequently settling down on the substrate surface after some oscillations (i.e., deposition). In addition, rings or waves around the periphery of the nanofluid droplets can be seen e.g., images at $t = 4$ ms. According to Chandra and Avedisian,[8] such rings could be formed due to the compression of liquid during impact. Figure 3 clearly shows that the spreading of nanofluid droplet at higher volume fraction ($\phi_{np} = 0.05$) is larger compared to droplet at lower volume fraction ($\phi_{np} = 0.01$). This is mainly because nanofluid with higher volume fraction of nanoparticles has larger kinetic energy (due to higher number density of nanoparticles) than that of the lower volume-fractioned nanofluid and thus can enhance the droplet spreading.

Experimental results for the effect of nanoparticle concentration on dimensionless spreading diameter and height of nanofluid droplet as a function of nondimensional time (t^*) are presented in Figures 4 and 5, respectively. The nanoparticles volume fraction is found to have significant influence on the spreading characteristics of droplets on solid surface. Figure 4 shows that except for $\phi_{np} = 0.05$, the maximum spreading diameters for all other concentrations of nanoparticles typically confined within $t^* < 6$. It can be demonstrated from Figure 4 that besides overall larger dimensionless diameter, droplet with higher nanoparticle volume fraction have higher peak spread compared to droplet with lower volume-fractioned nanofluid.

Results show that droplets first reach a maximum spread followed by the minimum spread (rebound) and then reach stability after oscillations for some moments. It is also observed that the droplet of lower volume-fractioned nanofluid takes a little shorter time to stabilize compared to droplet of higher volume-fractioned nanofluid. The lower peak could have contributed to this shorter stabilization time as less movement is required to reach the stable state. Since higher volume-fractioned nanofluid contains more nanoparticles per volume than that of lower volume fraction, according to a study by Wasan and Nikolov[22] there is better in-layer structuring of nanoparticles which might be the reason for larger spread of droplets for higher particle concentration observed in this study. Without elaborating Duursma et al.[23] also indicated that nanoparticle concentration may influence on the spreading of droplet. On the other hand, Figure 5 shows that the general trend of transient nondimensional heights of all droplets are fairly similar except the droplet for $\phi_{np} = 0.05$ where rebounding (i.e., increasing the droplet height) and stabilization of droplet take slightly longer time than those for other

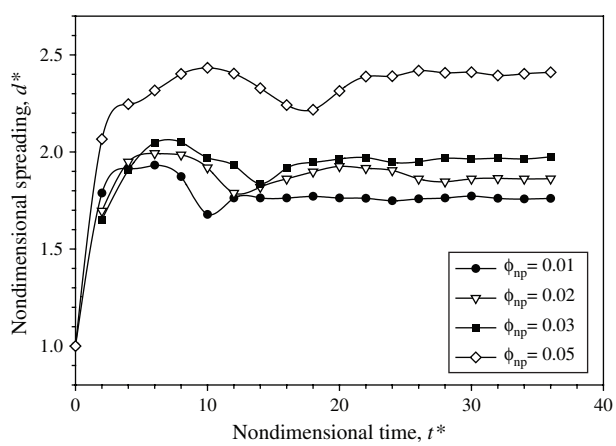

Fig. 4. Effect of nanoparticle volume fraction on nondimensional spreading diameter of nanofluid droplets with respect to dimensionless time at constant releasing height of 10 cm and surface temperature of 130 °C.

RESEARCH ARTICLE

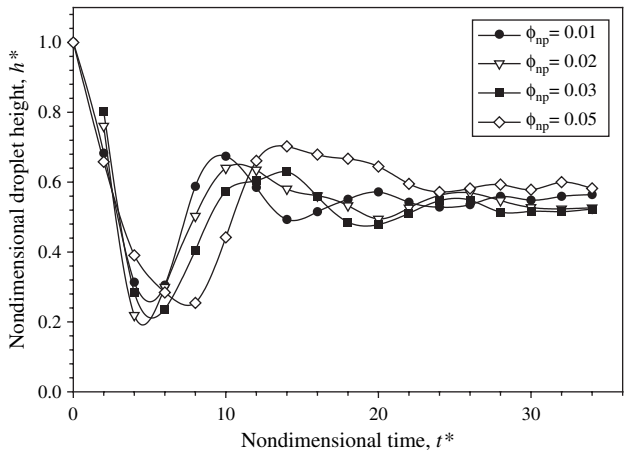

Fig. 5. Effect of nanoparticle volume fraction on nondimensional height of nanofluid droplets with respect to dimensionless time at constant releasing height of 10 cm and at surface temperature of 130 °C.

lower concentrations. For single wall carbon nanotubes (SWCNT)/water-based nanofluids, a similar trend of transient dimensionless droplet heights at non-boiling surface condition was also observed by Shen et al.[24]

4.2. Effect of Substrate Temperature

Sequence of typical images of droplet impact and spreading process at two substrate temperatures are shown in Figure 6. Except one late rebounding at 70 °C (at $t = 24$ ms in Fig. 6(a)) the droplet impact and spreading phenomena are quite similar to droplet morphology shown in Figure 3. Figures 7 and 8 present results of the effect of substrate temperatures on nondimensional droplet spreading diameter and height at constant particle concentration ($\phi_{np} = 0.01$) and droplet releasing height ($s =$ 10 cm). Although the general trends of droplet spreading looks quite similar for all temperatures, the stable spreading diameter (d^*) of nanofluid droplet found to decrease with increasing substrate temperature (Fig. 7). At higher surface temperatures (i.e., at 130 °C and 170 °C) and at stable stage (at $t^* > 14$) the dimensionless spreading diameters are found to be more uniform and consistent than those at lower temperatures (i.e., 22 °C and 70 °C). It can be demonstrated from Figure 7 that for all surface temperatures spreading of droplets right after the impingement increase rapidly ($t^* < 6$) followed by drastic decrease and after initial fluctuations ($t^* > 14$), droplets spreading become steady for non-heating surface condition (22 °C) and fairly constant for heating conditions (at 70 °C, 130 °C and 170 °C). On the other hand, Figure 8 shows that dimensionless heights of the droplets drastically decrease for initial period (i.e., $t^* < 7$) and then increase for next few moments (i.e., $6 < t^* < 12$) before getting stable state. The surface temperature is also found to affect the first minimum nondimensional height of the droplets. The time difference between the peak height and the minimum height also varied directly with the surface temperature. With a higher temperature, it takes little longer time for the droplet to change from its minimum to peak value. However, at the stable stage ($t^* > 14$) the overall nondimensional droplet height increases with increasing surface temperature. This could be due to the decrease of droplet spreading for a given volume of droplet. From Figures 6 to 8 it can be concluded that with increasing substrate temperature the overall spreading diameter and height of nanofluid droplet significantly decreases and increases, respectively. Similar trends of transient spreading and heights of droplets of SWCNT/deionized water-based nanofluid were also observed by Shen et al.[24] at both non-heating (25 °C) and heating (87.1 °C) surface temperatures.

4.3. Effect of Weber Number

Weber number which is commonly used in bubbles or droplets formation, breakage of liquid jets, and also analyzing fluid or thin film flows, can be written as $We = (\rho D V_0^2)/\sigma$ where ρ is the fluid density, σ is the surface tension of the liquid, D is the pre-impact diameter, and V_0 is the impact velocity of the droplet. For initial zero velocity (just before releasing the droplet), this impact velocity can be expressed by $V_0 = \sqrt{2gs}$ where g is the gravitational acceleration and s is the released height. Thus the Weber number can be re-written as $We = (2gD\rho s)/\sigma$ which shows that for a fixed size (diameter) of droplet of any liquid, the Weber number is directly related to the droplet releasing height. In general, for large Weber number where the impact energy is high, the droplet might

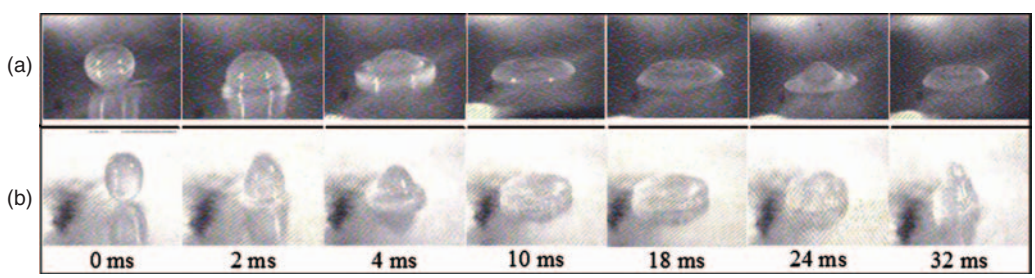

Fig. 6. Sequential droplet morphology of nanofluid at releasing height of 10 cm and $\phi_{np} = 0.01$ for surface temperatures of (a) 70 °C, (b) 130 °C.

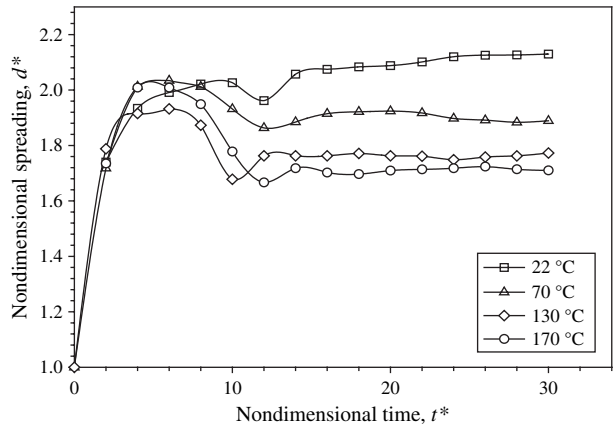

Fig. 7. Effect of substrate temperature on nondimensional spreading of nanofluid droplets as a function of dimensionless time at $\phi_{np} = 0.01$ and $s = 10$ cm.

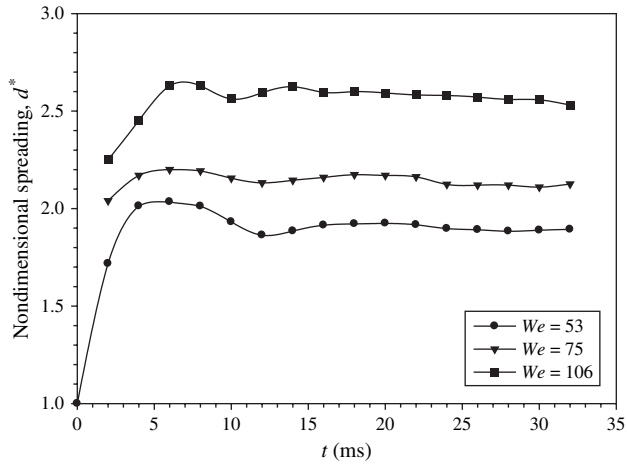

Fig. 9. Effect of weber number on sequential dimensionless spreading of nanofluid droplets at ϕ_{np} = 0.01 and at surface temperature of 130 °C.

shatter upon impact with the substrate surface whereas small Weber number might cause the liquid droplet sticking, spreading, or rebounding.

Figures 9 and 10 present results of sequential spreading characteristics of nanofluid droplet for the three different Weber numbers. It is noted that the nondimensional time, $t^* = tV_0/D$ is not used in this case due to different impact velocities (V_0) for different Weber numbers. As can be seen from Figure 9, at the largest Weber number ($We = 106$) droplets encountered the widest spread. This is because the droplet with the larger Weber number has a greater impact kinetic energy due to larger velocity that forces the droplet to spread out more upon contact with the substrate surface. The larger the Weber number, the larger the overall spreading diameter of droplets (Fig. 9). Duursma et al.[23] also reported that maximum droplet spreading ratio increases with increasing Weber number.

On the other hand, Figure 10 demonstrates that the overall dimensionless droplet height decreases with increasing Weber number. Due to the greater initial impact of the droplet with larger Weber number, the initial fluctuation in dimensionless height of the droplet ($t < 14$–16 ms) is much lower compared to droplet with smaller Weber number (Fig. 10). As mentioned previously, the kinetic energy of the droplet with larger Weber number is almost fully dissipated and leaves very less to propel them off the surface. However, the range from peak to minimum height for the droplets at smaller Weber number is larger than that of larger Weber number at which the droplets are not deformed severely upon impact resulting in small rise in the height. Droplet with large Weber number has large spread and with the large spread, the droplet is unable to rebound and rise greatly. The droplet could not overcome the high initial momentum, which is converted mostly to kinetic energy of the droplet to spread outward and to rebound upward. Nevertheless, present results clearly

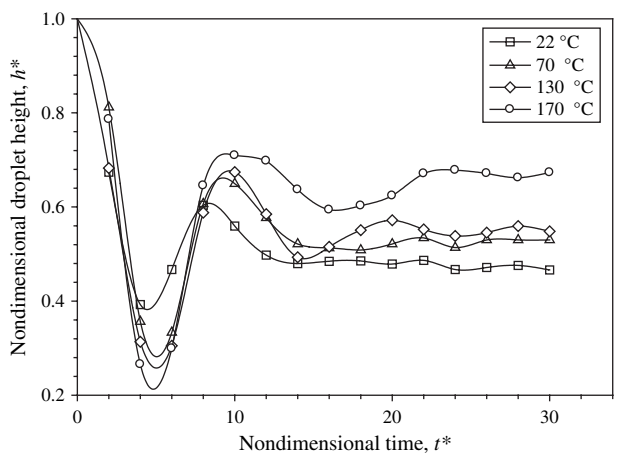

Fig. 8. Effect of substrate temperature on nondimensional height of nanofluid droplets as a function of dimensionless time at $\phi_{np} = 0.01$ and $s = 10$ cm.

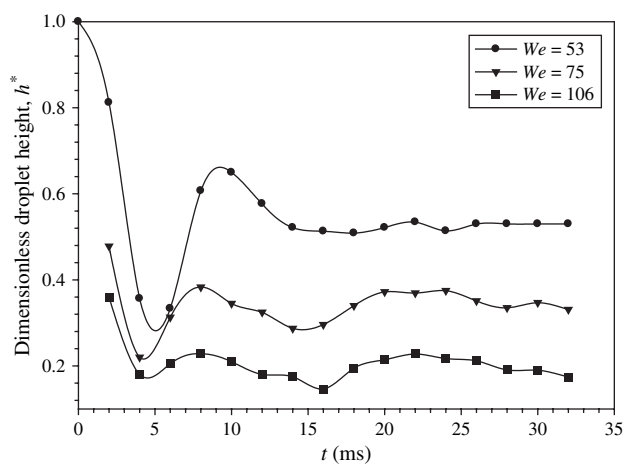

Fig. 10. Effect of weber number on sequential dimensionless height of nanofluid droplets at $\phi_{np} = 0.01$ and at surface temperature of 130 °C.

demonstrate that the Weber number significantly influences the spreading characteristics of nanofluid droplet (Figs. 9 and 10).

In this study, four distinct sequential regimes of droplet spreading namely initial spreading (drastic increase of spreading diameter, d from minimum to maximum or decrease of h from maximum to minimum), rebounding (drastic decrease of d from maximum to minimum or drastic increase of h from minimum to maximum after initial spreading), re-spreading (further increase of d or decrease of h after rebounding), and stable or equilibrium stage (steady spreading or constant) are observed and such spreading characteristics of nanofluid droplet is not well-understood at this stage. It is however believed that nanoparticles dispersed in the nanofluid droplet play important role in its spreading characteristics through nanofluid's properties (e.g., surface tension) as well as Brownian motion of nanoparticles.

5. CONCLUSIONS

The effects of several key factors such as nanoparticle volume fraction, substrate temperature, and Weber number on the spreading characteristics of nanofluid droplets impinging on aluminum substrate surface are studied experimentally.

The higher the volume fraction of nanoparticles the larger the spreading diameter of nanofluid droplet. The reason could be that the higher volume-fractioned nanofluid has better in-layer nanoparticle structuring which can promote enhancing the spreading of droplet on solid surface. The droplet of lower volume-fractioned nanofluid is also found to stabilize faster than that of higher volume-fractioned nanofluid. In addition, present results confirm that with increasing substrate temperature, the spreading diameter and height of nanofluid droplet considerably decreases and increases, respectively. Whereas, with increasing the Weber number the spreading diameter and height of nanofluid droplet are found to increase and decrease, respectively as the magnitude of the initial momentum and impact, which are directly related to the droplet releasing height (thus the Weber number), greatly influence the spreading dynamics of the droplet.

From the present experiments, it can be inferred that the volumetric concentration of nanoparticles, substrate surface temperature, and the Weber number significantly affect the spreading diameter and height of the impacted nanofluid droplets in different ways and nanofluid shows great promise for potential cooling techniques and applications, particularly in spray cool systems. Further investigations are imperative for better understanding and identifying spreading mechanisms of nanofluid droplets on solid under various droplet and surface conditions.

References and Notes

1. S. U. S. Choi, Developments and Applications of Non-Newtonian Flow, edited by D. A. Siginer and H. P. Wang, ASME, New York **(1995)**, Vol. FED 231/MD 66, p. 99.
2. X. Wang, X. Xu, and S. U. S. Choi, *J. Thermophys. Heat Transfer* 13, 474 **(1999)**.
3. J. A. Eastman, S. U. S. Choi, S. Li, W. Yu, and L. J. Thompson, *Appl. Phys. Lett.* 78, 718 **(2001)**.
4. J. A. Eastman, S. R. Phillpot, S. U. S. Choi, and P. Keblinski, *Annu. Rev. Mater. Res.* 34, 219 **(2004)**.
5. S. M. S. Murshed, K. C. Leong, and C. Yang, *Int. J. Therm. Sci.* 44, 367 **(2005)**.
6. W. Yu, D. M. Frances, J. L. Routbort, and S. U. S. Choi, *Heat Transfer Eng.* 29, 432 **(2008)**.
7. S. M. S. Murshed, K. C. Leong, and C. Yang, *Appl. Therm. Eng.* 28, 2109 **(2008)**.
8. S. Chandra and C. T. Avedisian, *Proc. R. Soc. Lond. A* 432, 13 **(1991)**.
9. N. Hatta, H. Fujimoto, and H. Takuda, *J. Fluid. Eng.* 117, 394 **(1995)**.
10. J. D. Bernardin, C. J. Stebbins, and I. Mudawar, *Int. J. Heat Mass Transfer* 40, 247 **(1997)**.
11. H. Y. Kim and J. H. Chun, *Phys. Fluids* 13, 643 **(2001)**.
12. W. M. Healy, J. G. Hartley, and S. I. Abdel-Khalik, *Int. J. Heat Mass Transfer* 44, 235 **(2001)**.
13. S. G. Kandlikar and M. E. Steinke, *Chem. Eng. Res. Des.* 79, 491 **(2001)**.
14. S. L. Manzello and J. C. Yang, *Int. J. Heat Mass Transfer* 47, 1701 **(2004)**.
15. A. L. Yarin, *Annu. Rev. Fluid Mech.* 38, 159 **(2006)**.
16. S. M. You, J. H. Kim, and K. H. Kim, *Appl. Phys. Lett.* 83, 3374 **(2003)**.
17. D. Wen and Y. Ding, *J. Nanoparticle Res.* 7, 265 **(2005)**.
18. H. D. Kim, J. Kim, and M. H. Kim, *Int. J. Multiphase Flow* 33, 691 **(2007)**.
19. Z. H. Liu and Y. H. Qiu, *Heat Mass Transfer* 43, 699 **(2007)**.
20. J. D. Bernardin, I. Mudawar, C. B. Walsh, and E. I. Franses, *Int. J. Heat Mass Transfer* 40, 1017 **(1997)**.
21. D. R. Heine, G. S. Grest, and E. B. Webb, *Phys. Rev. Lett.* 95, 107801 **(2005)**.
22. D. T. Wasan and A. D. Nikolov, *Nature* 423, 156 **(2003)**.
23. G. Duursma, K. Sefiane, and A. Kennedy, *Heat Transf. Eng.* 30, 1108 **(2009)**.
24. J. Shen, J. A. Liburdy, D. V. Pence, and V. Narayanan, *J. Phys.: Condens. Matter* 21, 464133 **(2009)**.
25. D. R. Lide, CRC Handbook of Chemistry and Physics, Taylor and Francis, Boca Raton, Florida **(2007)**.
26. S. M. S. Murshed, S. H. Tan, and N. T. Nguyen, *J. Phys. D: Appl. Phys.* 41, 085502 **(2008)**.

Received: 21 June 2010. Accepted: 14 July 2010.